EGFR Kinase Regulates Volume-sensitive Chloride Current Elicited by Integrin Stretch via PI-3K and NADPH Oxidase in Ventricular Myocytes

David M. Browe[1] and Clive M. Baumgarten[1,2]

[1]Department of Physiology and [2]Department of Internal Medicine (Cardiology), and the Pauley Heart Center, Medical College of Virginia, Virginia Commonwealth University, Richmond, Virginia 23298

Stretch of β1 integrins activates an outwardly rectifying, tamoxifen-sensitive Cl^- current (Cl^- SAC) via AT1 receptors, NADPH oxidase, and reactive oxygen species, and Cl^- SAC resembles the volume-sensitive Cl^- current ($I_{Cl,swell}$). Epidermal growth factor receptor (EGFR) kinase undergoes transactivation upon stretch, integrin engagement, and AT1 receptor activation and, in turn, stimulates NADPH oxidase. Therefore, we tested whether Cl^- SAC is regulated by EGFR kinase signaling and is volume sensitive. Paramagnetic beads coated with mAb for β1 integrin were attached to myocytes and pulled with an electromagnet. Stretch activated a Cl^- SAC that was 1.13 ± 0.10 pA/pF at +40 mV. AG1478 (10 μM), an EGFR kinase blocker, inhibited 93 ± 13% of Cl^- SAC, and intracellular pretreatment with 1 μM AG1478 markedly suppressed Cl^- SAC activation. EGF (3.3 nM) directly activated an outwardly rectifying Cl^- current (0.81 ± 0.05 pA/pF at +40 mV) that was fully blocked by 10 μM tamoxifen, an $I_{Cl,swell}$ blocker. Phosphatidylinositol 3-kinase (PI-3K) is downstream of EGFR kinase. Wortmannin (500 nM) and LY294002 (100 μM), blockers of PI-3K, inhibited Cl^- SAC by 67 ± 6% and 91 ± 25% respectively, and the EGF-induced Cl^- current also was fully blocked by LY294002. Furthermore, gp91ds-tat (500 nM), a cell-permeable, chimeric peptide that specifically blocks NADPH oxidase assembly, profoundly inhibited the EGF-induced Cl^- current. Inactive permeant and active impermeant control peptides had no effect. Myocyte shrinkage with hyperosmotic bathing media inhibited the Cl^- SAC and EGF-induced Cl^- current by 88 ± 9% and 127 ± 11%, respectively. These results suggest that β1 integrin stretch activates Cl^- SAC via EGFR, PI-3K, and NADPH oxidase, and that both the Cl^- SAC and the EGF-induced Cl^- currents are likely to be the volume-sensitive Cl^- current, $I_{Cl,swell}$.

The Journal of General Physiology

INTRODUCTION

Integrins are transmembrane heterodimeric receptors that transmit force from the extracellular matrix to the cytoskeleton and activate multiple signaling cascades. The β1D-splice variant is the principal integrin isoform expressed in adult mammalian heart (Zhidkova et al., 1995). We have shown that specific stretch of β1 integrin in ventricular myocytes under isosmotic conditions activates an outwardly rectifying Cl^- current (Cl^- SAC) (Browe and Baumgarten, 2003, 2004) that resembles the volume-sensitive Cl^- current, $I_{Cl,swell}$ (Sorota, 1992; Tseng, 1992). Cl^- SAC, like $I_{Cl,swell}$, contributes to the background current, activates slowly over several minutes, exhibits outward rectification, partially inactivates at positive potentials, and is blocked by tamoxifen. Regulation of Cl^- SAC involves Src and/or focal adhesion kinase (FAK), angiotensin AT1 receptors, and reactive oxygen species (ROS) generated, at least in part, by NADPH oxidase. Furthermore, angiotensin II (AngII) and H_2O_2 each elicit Cl^- SAC in ventricular myocytes in the absence of stretch (Browe and Baumgarten, 2004).

Stretch (Oeckler et al., 2003), integrins (Moro et al., 2002), and AT1 receptors (Shah and Catt, 2003) transactivate epidermal growth factor receptor (EGFR) kinase, a member of the ErbB family of receptor tyrosine kinases (RTKs). Unstimulated EGFR kinase is a monomer consisting of an extracellular ligand binding domain, a single membrane spanning domain, and a cytoplasmic kinase domain (Holbro and Hynes, 2004). With ligand binding, EGFR kinase dimerizes, transautophosphorylates six specific tyrosines within its noncatalytic cytoplasmic tail, and translocates from caveolae to costameres (Shah, 2002). EGFR kinase then recruits and phosphorylates various adaptor and signaling molecules that bind phosphotyrosine motifs with their SH2 and PTB domains and serves as a platform for integrating downstream signaling.

Signaling by EGFR kinase and AT1 receptors is mediated by phosphatidylinositol 3-kinase (PI-3K), a family of lipid kinases also activated by integrins, stretch, and H_2O_2 (Ushio-Fukai et al., 1999; Oudit et al., 2004). The best characterized PI-3K are heterodimers composed

Correspondence to Clive M. Baumgarten: clive.baumgarten@vcu.edu

Abbreviations used in this paper: AngII, angiotensin II; Cl^- SAC, stretch-activated Cl^- current; DPI, diphenyleneiodonium; EGF, epidermal growth factor; EGFR, EGF receptor; FAK, focal adhesion kinase; HB-EGF, heparin-binding EGF; PI-3K, phosphatidylinositol 3-kinase; PtdIns(3,4)P_2, phosphatidylinositol 3,4 bisphosphate; PtdIns(3,4,5)P_3, phosphatidylinositol 3,4,5-triphosphate; ROS, reactive oxygen species; RTK, receptor tyrosine kinase.

of a p110 catalytic subunit tightly coupled to a regulatory subunit. Cardiac myocytes principally express the p110α and γ isoforms that couple with the p85 and p101 regulatory subunits, respectively (Prasad et al., 2003; Oudit et al., 2004). The p110α-p85 and p110γ-p101 dimers are activated by interaction with phosphotyrosines or the βγ subunit of heterotrimeric G proteins, respectively, and catalyze inositol ring phosphorylation at the D-3 position to produce phosphatidylinositol 3,4,5-triphosphate (PtdIns(3,4,5)P_3) and phosphatidylinositol 3,4-bisphosphate (PtdIns(3,4)P_2), potent signaling molecules.

EGFR kinase and PI-3K also participate in the activation of NADPH oxidase (Seshiah et al., 2002; Vignais, 2002). Cardiac myocytes express a transmembrane flavocytochrome b_{558} complex consisting of gp91^{phox} (Nox2) and p22^{phox}, as well as the cytosolic components p47^{phox}, p67^{phox}, and Rac (Li et al., 2002; Xiao et al., 2002; Heymes et al., 2003). Nox4, a homologue of gp91^{phox}, also is expressed (Byrne et al., 2003). NADPH oxidase activation involves translocation of the cytosolic components to the membrane and their assembly with flavocytochrome b_{558} (Vignais, 2002). Once assembled, the NADPH oxidase complex uses intracellular NADPH as substrate to catalyze the single electron reduction of molecular O_2 to superoxide anion, $\cdot O_2^-$, which is subsequently converted to H_2O_2 by superoxide dismutase (SOD).

Assembly of the active NADPH oxidase requires the binding of gp91^{phox} to p47^{phox} (Vignais, 2002). Recently, a cell permeable, chimeric peptide that inhibits this interaction was developed (Rey et al., 2001). The inhibitor, gp91ds-tat, combines the 9-mer gp91^{phox} docking sequence for p47^{phox} with a 9-mer from the HIV tat sequence that mediates membrane permeation. gp91 ds-tat can be used to selectively evaluate the role of NADPH oxidase in regulating Cl^- SAC without affecting ROS production at other sites, such as the flavocytochromes within the mitochondria.

The aim of this study was to examine the role of EGFR kinase, PI-3K, and NADPH oxidase in the activation of Cl^- SAC in ventricular myocytes and to determine whether Cl^- SAC is volume sensitive. Paramagnetic beads coated with anti–β1 integrin mAb were used to stretch integrins. Block of EGFR kinase or PI-3K during stretch inhibited Cl^- SAC. Moreover, exogenous epidermal growth factor (EGF) fully activated Cl^- SAC, and the EGF-induced current was inhibited by PI-3K and NADPH oxidase blockers and by tamoxifen, a blocker of $I_{Cl,swell}$. Finally, Cl^- SAC elicited by either integrin stretch or exogenous EGF was volume sensitive and was completely inhibited by osmotic shrinkage. Thus, the Cl^- SAC and EGF-induced Cl^- current are likely to be carried by the same channel as $I_{Cl,swell}$. A preliminary report appeared previously (Browe and Baumgarten, 2005b).

MATERIALS AND METHODS

Ventricular Myocyte Isolation

Left ventricular myocytes were freshly isolated from adult New Zealand white rabbits (~3 kg) of either gender. Hearts were excised, attached to a Langendorff perfusion apparatus, and subjected to an enzymatic dissociation procedure described previously (Browe and Baumgarten, 2003). Isolated myocytes were washed and stored in a modified KB medium. All experimental recordings were conducted within 10 h of myocyte isolation. Single myocytes chosen for study were rod-shaped, quiescent, displayed clear striations, and were free of membrane blebs or other morphological irregularities.

Tyrode solution for cell isolation contained (in mM) 130 NaCl, 5 KCl, 1.8 $CaCl_2$, 0.4 KH_2PO_4, 3 $MgCl_2$, 5 HEPES, 15 taurine, 5 creatine, 10 glucose, pH 7.25 (adjusted with NaOH). $CaCl_2$ was replaced with 0.1 mM Na_2-EGTA to make Ca^{2+}-free Tyrode solution. Enzyme solution contained 1.5–1.75 mg/ml BSA (Sigma-Aldrich; A7906), 0.5 mg/ml collagenase (type II, Worthington), and 0.05 mg/ml pronase (Sigma-Aldrich; type XIV) in nominally Ca^{2+}-Tyrode solution without EGTA. All isolation solutions were well oxygenated and maintained at 37°C. Modified KB medium contained (in mM) 120 K-glutamate, 10 KCl, 10 KH_2PO_4, 0.5 K_2-EGTA, 10 taurine, 1.8 $MgSO_4$, 10 HEPES, 20 glucose, 10 mannitol, pH 7.2 (adjusted with KOH).

Experimental Solutions and Drugs

Single ventricular myocytes were scattered on a poly-L-lysine–coated, glass-bottomed chamber and placed on the stage of an inverted microscope (Diaphot; Nikon). Hoffman modulation optics (×40; NA = 0.55) and a high resolution TV camera (CCD72; Dage-MTI) were used to visualize the cells. Bath solution designed to isolate anion currents was suprafused at 2–3 ml/min and contained (in mM) 145 *N*-methyl-D-glucamine (NMDG)-Cl, 4.3 $MgCl_2$, 10 HEPES, 5 glucose, pH 7.4 (adjusted with NMDG). Pipette solution contained (in mM) 110 Cs-aspartate, 20 CsCl, 2.5 Mg-ATP, 8 Cs_2-EGTA, 0.1 $CaCl_2$, 10 HEPES, pH 7.1 (adjusted with CsOH; liquid junction potential, −13.2 mV). Pipette free-Ca^{2+} was estimated to be ~35 nM (WinMAXC 2.4; www.stanford.edu/~cpatton/maxc.html). All recordings were made at room temperature (22°C–23°C).

The tyrphostin AG1478 (1 mM; Calbiochem), tamoxifen (20 mM; Sigma-Aldrich), wortmannin (1 mM, Calbiochem), and LY294002 (50 mM, Calbiochem) were prepared as stock solutions in DMSO at the indicated concentrations and kept frozen (−20°C) in small aliquots until use. EGF (mouse; Calbiochem) was dissolved directly in bath solution and kept frozen (−20°C) in small aliquots until use at a final concentration of 3.3 nM, which is equivalent to 20 ng/ml. A membrane-permeant inhibitor of NADPH oxidase, gp91ds-tat, an inactive membrane-permeant analogue, scramb-tat, and an active but impermeant gp91ds peptide were synthesized by the Tufts University Core Facility, as previously described by others (Rey et al., 2001). The inhibitor, gp91ds-tat, is a fusion peptide made from a 9-mer, CSTRIRRQL, that inhibits assembly of NADPH oxidase by mimicking the gp91^{phox} docking site for the cytoplasmic p47^{phox} subunit and a 9-mer from the tat HIV coat protein that confers membrane permeability. The gp91^{phox} docking site sequence is identical in a number of experimental species including rabbit (Gauss et al., 2002), but experimental evidence and homology suggest that gp91ds-tat may not distinguish between gp91^{phox} homologues (Rey et al., 2001). The inactive fusion peptide, scramb-tat, was made by scrambling the 9-mer docking peptide to minimize matches in the GenBank/EMBL/DDBJ database, whereas gp91ds is the docking site 9-mer without tat and is active in broken cell systems. Each peptide was prepared as stock solutions (1.2 mg/ml) in 150 mM NaCl

acidified with 10 mM acetic acid and kept frozen (−20°C) in small aliquots until use. For certain experiments, bath solution osmolarity was increased from 300 mosmol/kg (1T) to 450 mosmol/kg (1.5T) by addition of mannitol, preserving a constant ionic strength.

Integrin Stretch

Force was applied directly and specifically to β1 integrins using mAb-coated paramagnetic beads and an electromagnet, as previously described (Browe and Baumgarten, 2003). mAb for the β1 subunit of integrin (MAB2250, IgG_1; Chemicon) was attached by anti–pan IgG mAb to the surface of uniform 4.5 ± 0.2 μm diameter (mean ± SD) superparamagnetic beads containing iron oxides (dynabeads M-450 pan mouse IgG; Dynal Biotech). Anti-β1 integrin mAb–coated beads were added to myocytes in the bath and were permitted to randomly settle on myocytes from above while the flow of bath solution was turned off. After ~5 min, unbound beads were washed away by restoring flow. Myocytes chosen for study typically had three to five coated beads on their surface, and presumably, each bead was bound to multiple β1 integrins.

A water-cooled electromagnet was placed directly on top of the bath, and patch pipettes were passed through an opening at the base of the coil. Current through the coil was set to generate a magnetic flux density of 35 Gauss (G) and a magnetic flux density gradient of 2,400 G/m that was uniform in the x–y plane occupied by the myocytes on the chamber floor. The resulting force vector imposed on each bead was directed upwards toward the coil, perpendicular to the long axis of the myocyte, and was estimated to have a magnitude of 1.2 pN/bead (Browe and Baumgarten, 2003).

Electrophysiological Recordings

Pipettes were pulled from 7740 thin-walled borosilicate glass capillary tubing (Sutter) and fire polished to give a final tip diameter of 3–4 μm and resistance in bath solution of 2–3 MΩ. Membrane currents were recorded with an EPC-7 amplifier (List-Medical) using the whole cell configuration. A 150 mM KCl agar bridge served as the ground electrode. Seal resistances of 5–30 GΩ were typically obtained. Membrane potential was corrected for the measured liquid junction potential before forming a seal. After seal formation, the membrane patch was ruptured by application of negative pressure or by a brief zapping pulse. Myocytes were dialyzed for at least 10 min before recordings commenced. Voltage clamp protocols and data acquisition were governed by a Digidata 1200B or 1322A and pClamp 8.0 (Axon Instruments). Successive 500-ms voltage steps were taken from a holding potential of −60 mV to test potentials ranging from −100 to +40 mV in +10 mV increments. Membrane currents were low-pass filtered at 2 kHz (8-pole Bessel 902, Frequency Devices) and digitized at 10 kHz. For presentation, selected records were low-pass filtered at 50 Hz post-digitization with a Gaussian filter in PClamp. Cl^- currents exhibited strong voltage-dependent inactivation, and isochronal IV curves were plotted based on the average current recorded 20–35 ms after the onset of the voltage step.

Statistics

Data are reported as mean ± SEM; *n* denotes the number of cells. Mean currents are expressed as current density (pA/pF) to account for differences in myocyte surface membrane area, and paired comparisons usually are expressed as a percentage. Statistical analyses were performed by SigmaStat 3.1 (Systat). For multiple comparisons, a one-way repeated measures ANOVA was performed and was followed by a Student-Newman-Keuls test. For comparisons of two groups, a one-tailed paired Students *t* test was conducted. In both cases, $P < 0.05$ was taken as significant.

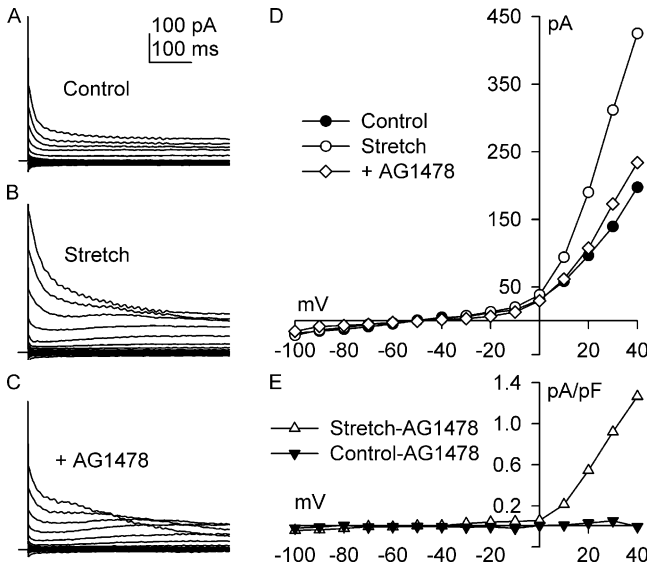

Figure 1. AG1478, a specific EGFR kinase blocker, inhibits Cl^- SAC but does not affect background current in the absence of stretch. Families of currents recorded before (A, Control) and after (B, Stretch) activation of Cl^- SAC by β1 integrin stretch (5 min), and after addition of AG1478 (10 μM, 10 min) to the bath with continued stretch (C, +AG1478). Holding potential, −60 mV; test potentials, −100 to +40 mV; step duration, 500 ms. Horizontal bar denotes 0 current. (D) I-V relationships for A–C; each reversed near −50 mV (E_{Cl} = −52 mV). (E) I-V relationships comparing AG1478-sensitive current after stretch (Stretch-AG1478) and the AG1478-sensitive background current (Control-AG1478) in the absence of stretch in different myocytes. At +40 mV, stretch-induced Cl^- current was 1.13 ± 0.10 pA/pF, and AG1478 reduced Cl^- SAC by 93 ± 13% (n = 4, P = 0.001) but did not affect background current (n = 4; P = 0.526) in unstretched myocytes.

RESULTS

EGFR Kinase Participates in Cl^- SAC Activation

Integrins, AT1 receptors, and mechanical stretch initiate transactivation of EGFR kinase (Moro et al., 2002; Oeckler et al., 2003; Shah and Catt, 2003). Because EGFR kinase serves as a nexus for integrating diverse stimuli that regulate Cl^- SAC, we assessed its role in the response to β1 integrin stretch. Fig. 1 illustrates families of anion currents at test potentials between −100 and +40 mV and the corresponding I–V relationships. Under control conditions with anti-β1 integrin mAb–coated paramagnetic beads attached to the myocyte surface but before the application of integrin stretch, a small outwardly rectifying background current that partially inactivated at positive potentials was present (Fig. 1 A). The background current reversed at −49 mV, which is near the calculated value of −52 mV for E_{Cl} (Fig. 1 D). Partial activation of $I_{Cl,swell}$ is thought to occur under these conditions, and the background Cl^- current is sensitive to the $I_{Cl,swell}$ blocker tamoxifen (Hume et al., 2000). Consequently, $I_{Cl,swell}$ is likely to comprise much of the background Cl^- current observed in 1T. Stretch

of β1 integrins progressively increased the magnitude of the outward Cl^- current over 5 min, giving a more than twofold augmentation of outward current at +40 mV in this example (Fig. 1, B and D). After full activation by stretch, the Cl^- current partially inactivated at positive potentials, and its I–V relationship showed strong outward rectification and reversed near E_{Cl}, as previously shown (Browe and Baumgarten, 2003, 2004).

Block of EGFR kinase with 10 μM AG1478, a selective inhibitor (Levitzki and Gazit, 1995), almost completely abrogated the stretch-induced Cl^- current in the continued presence of integrin stretch (Fig. 1, C and E). The I–V relationship was nearly restored to its control level after 10 min, and the reversal potential was unaffected. Overall, integrin stretch increased the Cl^- current at +40 mV from 1.33 ± 0.07 to 2.30 ± 0.22 pA/pF, and exposure to AG1478 (10–12 min) with continued integrin stretch reduced the current to 1.46 ± 0.17 pA/pF (n = 4). Thus, block of EGFR kinase inhibited 93 ± 13% (n = 4, P = 0.001) of stretch-induced current at +40 mV, and the current after block was not significantly different from the control current (n = 4, P = 0.385). Neither stretch of β1 integrin nor subsequent AG1478 application significantly altered inward current at −100 mV, however, as also was shown for stretch (Browe and Baumgarten, 2003, 2004).

As a control, we examined the effect of AG1478 (10 μM, 10 min) on the background Cl^- current in the absence of integrin stretch. In contrast to its pronounced inhibitory effect on the stretch-induced outward current, AG1478 did not significantly alter the background Cl^- current (Fig. 1 E) at either +40 mV (n = 4; P = 0.526) or −100 mV (n = 4; P = 0.306).

AG1478 also prevented activation of Cl^- SAC when it was applied intracellularly before integrin stretch. Myocytes were pretreated by including 1 μM AG1478, a 10-fold lower concentration, in the pipette solution. After 15–20 min of dialysis, myocytes were stretched for 10 min, a time sufficient to fully activate Cl^- SAC (Browe and Baumgarten, 2003). After pretreatment, stretch elicited a small but statistically insignificant current, 0.23 ± 0.14 pA/pF, at +40 mV (n = 5, P = 0.10). This current was only 23% of that observed without pretreatment, 0.97 ± 0.09 pA/pF (n = 18).

Exogenous EGF Activates Cl^- SAC

If transactivation of EGFR kinase is an upstream signaling event in the activation of Cl^- SAC, exogenous EGF, which binds EGFR kinase and stimulates FAK and Src activity and ROS production (Brunton et al., 1997; Park et al., 2004), might be expected to mimic the effect of integrin stretch. Fig. 2 illustrates the effect of exogenous EGF on Cl^- currents in the absence of integrin stretch. Under control conditions, a typical background current was observed (Fig. 2, A and E). Addition of 3.3 nM EGF to bathing solution for 6 min evoked an outwardly

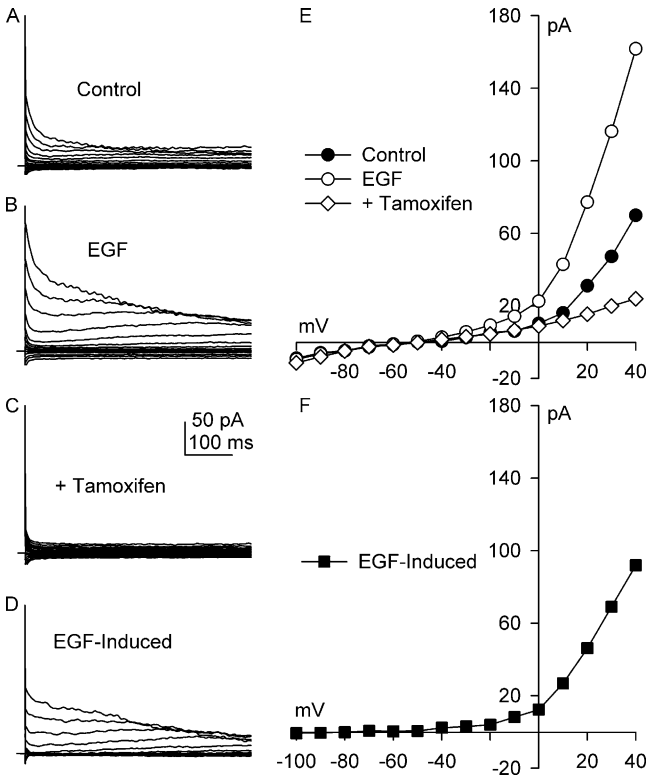

Figure 2. Exogenous EGF activates Cl^- current in the absence of integrin stretch. Currents before (A, Control) and after (B, EGF) exposure to EGF (3.3 nM, 6 min), and after addition of the Cl^- SAC and $I_{Cl,swell}$ blocker tamoxifen (10 μM, 6 min) in the continued presence of EGF (C, +Tamoxifen). EGF-induced difference current (D, EGF-Induced) was obtained by digital subtraction. I-V relationships for A-C (E) and for the EGF-induced current (F). Each I-V relationship reversed near E_{Cl}. The EGF-induced Cl^- current partially inactivated at positive potentials, exhibited strong outward rectification, and both the EGF-induced and background Cl^- currents were completely blocked by tamoxifen. At +40 mV, the Cl^- current elicited by EGF was 0.81 ± 0.05 pA/pF (n = 24, P < 0.001), and tamoxifen reduced the current by 170 ± 8% (n = 4, P < 0.001).

rectifying Cl^- current that exhibited partial inactivation at positive potentials (Fig. 2, B and E). The EGF-induced difference current (Fig. 2, D and F) was obtained by digital subtraction. Overall, exogenous EGF (5–6 min) increased the outward Cl^- current at +40 mV by 0.81 ± 0.05 pA/pF (n = 24, P < 0.001), from 1.20 ± 0.07 to 2.01 ±0.08 pA/pF. As found with stretch, EGF had a very modest effect on the inward Cl^- current. At −100 mV, EGF increased inward current by 0.04 ± 0.01 pA/pF (n = 24; P < 0.001), from −0.24 ± 0.02 to −0.28 ± 0.03 pA/pF. Significant effects of EGF on inward current were not consistently detected in smaller groups, however.

To further characterize the EGF-induced current, we examined its sensitivity to tamoxifen. Tamoxifen inhibits Cl^- SAC and $I_{Cl,swell}$ but does not affect either the PKA-regulated CFTR or the Ca^{2+}-activated Cl^- currents (Hume et al., 2000; Browe and Baumgarten, 2003). After full activation of Cl^- current by 3.3 nM EGF,

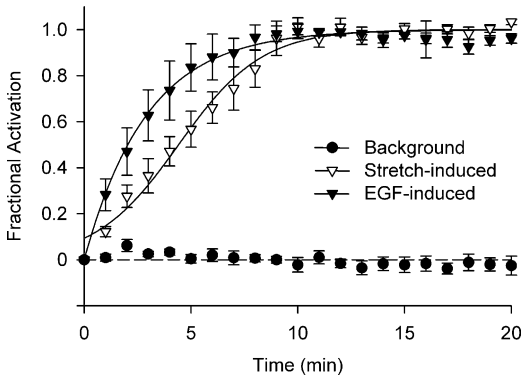

Figure 3. Time courses of Cl^- currents activated by EGF (3.3 nM) and integrin stretch and the background current. Currents at +40 mV were recorded at 1-min intervals for 20 min. Stretch- and EGF-induced currents were normalized by their steady-state values, 1.19 ± 0.07 (n = 4) and 0.91 ± 0.07 (n = 4), respectively, and the background current was normalized by the steady-state current after stretch. Cl^- current activation by EGF exhibited an exponential time course (τ = 3.2 ± 0.9 min; n = 4; equivalent $t_{1/2}$ = 2.2 ± 0.6 min), while activation by integrin stretch followed a slower, sigmoidal time course ($t_{1/2}$ = 4.3 ± 0.6 min; n = 4). The background current was nearly constant throughout the recording period in unstimulated myocytes. Solid lines are fits to averaged data; dashed line is zero current.

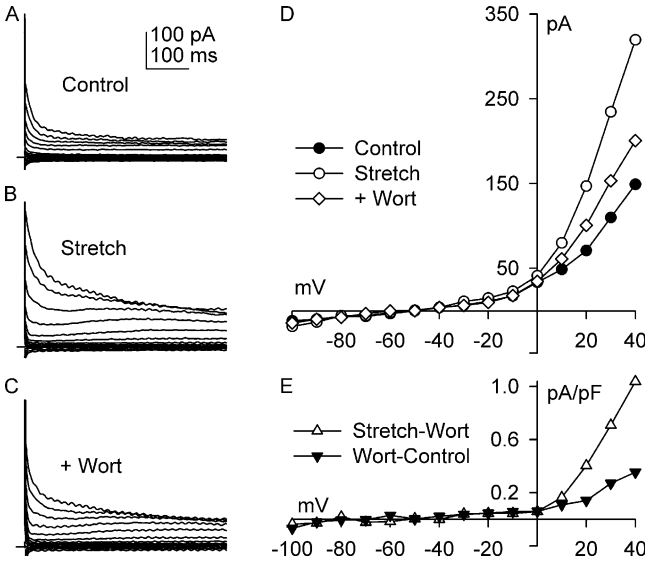

Figure 4. Wortmannin, a PI-3K blocker, partially inhibited Cl^- SAC. Currents before (A, Control) and after (B, Stretch) integrin stretch (6 min), and after exposure to wortmannin (500 nM, 12 min) with continued stretch (C, +Wort). (D) I-V relationships for A–C; each reversed near E_{Cl}. (E) I-V relationships comparing the wortmannin-sensitive current after integrin stretch (Stretch-Wort) and the wortmannin-sensitive background current (Wort-Control) in different myocytes. At +40 mV, wortmannin inhibited 67 ± 6% (n = 7; P < 0.001) of the Cl^- SAC. In contrast, wortmannin elicited a small increase in background current at +40 mV, 15 ± 5% (n = 4; P = 0.02), in unstretched myocytes.

exposure to 10 μM tamoxifen for 6 min in the continued presence of EGF completely abolished the EGF-induced Cl^- current as well as a large fraction of the background Cl^- current (Fig. 2, C and E). In these experiments, tamoxifen (6–8 min) blocked 170 ± 8% (n = 4; P < 0.001) and 177 ± 55% (n = 4; P < 0.02) of the EGF-induced current at +40 and −100 mV, respectively. EGF increased the Cl^- current at +40 mV from 1.15 ± 0.09 to 1.85 ± 0.06 pA/pF (n = 4; P < 0.001), and tamoxifen reduced the current to 0.67 ± 0.13 pA/pF, a value significantly less than control (n = 4; P < 0.01).

Fig. 3 compares the time course of Cl^- currents at +40 mV after activation by either EGF (3.3 nM) or integrin stretch, and as a control for time, the background current in the absence of an intervention. The EGF-induced Cl^- current was well described by a single exponential with a time constant of 3.2 ± 0.9 min (n = 4), equivalent to a $t_{1/2}$ of 2.2 ± 0.6 min, and was 0.91 ± 0.07 pA/pF at 20 min. Activation by integrin stretch was slower and sigmoidal with a $t_{1/2}$ of 4.3 ± 0.6 min (n = 4), and the steady-state current was 1.19 ± 0.07 pA/pF. Once activated, both currents remained at stable levels for the remainder of the recording period. In the absence of an intervention, the background current was stable for 20 min. The more rapid activation of Cl^- current by EGF as compared with stretch is consistent with, but does not prove, the idea that EGF is a downstream event in the stretch-induced signaling cascade regulating Cl^- SAC. Moreover, these data demonstrate the stability of the current recordings and serve as a time control for studies with blockers.

Role of PI-3K

Mechanical stretch, cell swelling, and integrin clustering all activate PI-3K (Sadoshima and Izumo, 1997; Franchini et al., 2000). Upon integrin clustering, activation of FAK and Src leads to the recruitment of PI-3K to costameres (Franchini et al., 2000), and PI-3K regulates NADPH oxidase activity (Vignais, 2002). Fig. 4 illustrates a test of the idea that PI-3K also participates in the activation of Cl^- SAC in response to β1 integrin stretch using wortmannin, an irreversible blocker of PI-3K (Stein and Waterfield, 2000). After activating Cl^- SAC by β1 integrin stretch for 6 min (Fig. 4, B and D), exposure to 500 nM wortmannin for 12 min with continued integrin stretch partially inhibited the outward Cl^- SAC (Fig. 4, C and D). Wortmannin (12–15 min) blocked 67 ± 6% (n = 7; P < 0.001) of the Cl^- SAC at +40 mV. Stretch increased the Cl^- current from 1.45 ± 0.14 to 2.47 ± 0.17 pA/pF, and wortmannin reduced the current to 1.81 ± 0.12 pA/pF (n = 7; P < 0.001). Although block of Cl^- SAC by wortmannin at +40 mV was substantial, the current remained significantly greater than control (n = 7; P = 0.006). Surprisingly, wortmannin (500 nM, 12 min) augmented the outward background current in the absence of stretch (Fig. 4 E). At +40 mV, the Cl^- current was increased by 15 ± 5% (n = 4; P = 0.02), from 1.16 ± 0.14 to 1.33 ± 0.16 pA/pF. The basis for the stimulation of background Cl^- current was not investigated further.

To verify the involvement of PI-3K in the response to integrin stretch, LY294002 was employed. LY294002 is structurally and mechanistically distinct from wortmannin and reversibly inhibits PI-3K (Stein and Waterfield, 2000; Oudit et al., 2004). Fig. 5 confirms the sensitivity of Cl^- SAC to block of PI-3K. After activating Cl^- SAC by β1 integrin stretch for 5 min, exposure to LY294002 (20 μM, 15 min) with continued stretch blocked almost all of the Cl^- SAC (Fig. 5, A and B). Stretch increased the current at +40 mV from 1.14 ± 0.28 to 1.86 ± 0.36 pA/pF (n = 4; P < 0.001), and LY294002 (20 μM, 15 min) reduced the current by 99 ± 11% (n = 4; P < 0.001). The current remaining in the presence of LY294002, 1.20 ± 0.35 pA/pF, was not significantly different from the control current (n = 4; P = 0.54). In contrast to its pronounced inhibition of the stretch-induced current, LY294002 (20 μM, 15 min) had a negligible effect on the background current in the absence of stretch (Fig. 5 C). At +40 mV, LY294002 reduced background current by only 3 ± 1% (n = 4; P = 0.07), from 0.62 ± 0.07 to 0.60 ± 0.08 pA/pF.

EGFR kinase also utilizes PI-3K as one of its principal downstream mediators of signaling (Bogdan and Klämbt, 2001). Therefore, we tested whether the Cl^- current elicited by exogenous EGF (3.3 nM, 6 min) also depended on PI-3K. LY294002 (20 μM, 12 min) inhibited almost all of the EGF-induced current in the continued presence of EGF. Overall, EGF increased the Cl^- current at +40 mV from 0.97 ± 0.10 to 1.66 ± 0.09 pA/pF, and LY294002 (20 μM, 12–14 min) blocked 124 ± 16% (n = 4; P < 0.001) of the current elicited by EGF. The current remaining after LY294002, 0.82 ± 0.14 pA/pF, was not significantly different from the control (n = 4; P = 0.15). The inward currents at −100 mV were small and were not significantly affected in this set of experiments. Thus, block of PI-3K by LY294002 had the same inhibitory effect on the EGF- and integrin stretch–induced Cl^- currents but no effect on the outwardly rectifying background current.

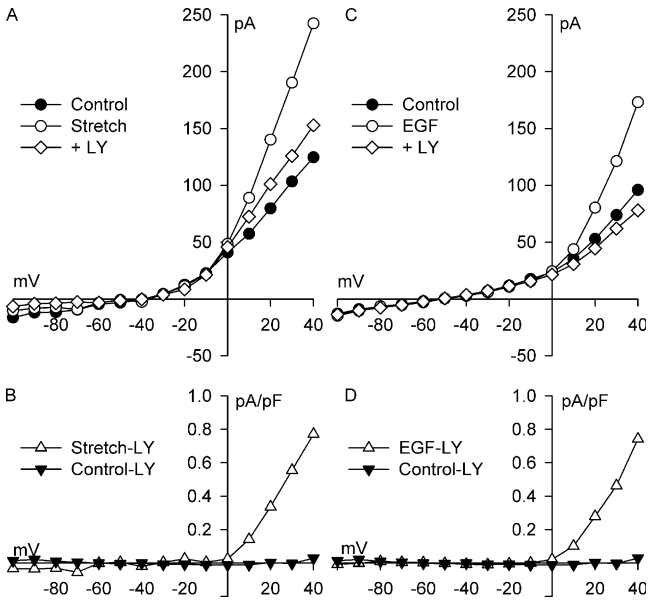

Figure 5. LY294002, a PI-3K blocker, completely inhibited stretch- and EGF-induced Cl^- current but did not affect background current. (A) I-V relationships before (Control) and after (Stretch) activation of Cl^- SAC by integrin stretch (5 min), and after exposure to LY294002 (20 μM, 15 min) with continued stretch (+LY). At +40 mV, LY294002 inhibited 99 ± 11% (n = 4, P < 0.001) of the stretch-induced Cl^- SAC. (B) I-V relationships comparing the LY294002-sensitive current (Stretch-LY) after stretch (5 min), and the LY294002-sensitive background current (Control-LY) in unstretched myocytes. (C) I-V relationships before (Control) and after (EGF) activation of Cl^- current with EGF (3.3 nM, 5 min), and after exposure to LY294002 (20 μM, 15 min) in the continued presence of EGF (+LY). At +40 mV, LY294002 inhibited 124 ± 16% (n = 4, P < 0.001) of the EGF-induced Cl^- current. (D) I-V relationships comparing the LY294002-sensitive current after EGF exposure (EGF-LY), and the LY294002-sensitive background current (Control-LY; from B). LY294002 did not significantly affect background current (n = 4; P = 0.07) in the absence of a stimulus.

Role of NADPH Oxidase in EGF-induced Cl^- Current

Previously we provided evidence that activation of Cl^- SAC by integrin stretch involves NADPH oxidase and the production of ROS (Browe and Baumgarten, 2004). EGFR kinase and PI-3K are known to participate in the activation of NADPH oxidase (Seshiah et al., 2002). As illustrated in Fig. 6, we tested whether the Cl^- current evoked by exogenous EGF also requires NADPH oxidase activity. First, Cl^- current was elicited with EGF (3.3 nM, 5 min; Fig. 6, B and D), and then gp91ds-tat, a selective membrane-permeant fusion peptide blocker of NADPH oxidase (Rey et al., 2001), was added. In the continued presence of EGF, gp91ds-tat (500 nM, 15 min) completely inhibited the EGF-induced Cl^- current (Fig. 6, C and D). EGF (3.3 nM, 5 min) increased outward Cl^- current at +40 mV from 1.16 ± 0.15 to 2.16 ± 0.16 pA/pF (n = 4; P < 0.001), and gp91ds-tat (500 nM, 12 – 15 min) inhibited 133 ± 20% (n = 4; P <0.001) of the EGF-induced Cl^- current. The current after gp91ds-tat treatment, 0.94 ± 0.07 pA/pF, was not significantly different from the control current (n = 4; P = 0.19). EGF also significantly increased the inward Cl^- current at −100 mV from −0.16 ± 0.02 to −0.23 ± 0.01 pA/pF (n = 4; P < 0.01), and gp91ds-tat reduced the current to −0.18 ± 0.01 pA/pF, blocking 87 ± 27% (n = 4; P = 0.01).

To rule out nonspecific effects of gp91ds-tat, experiments were conducted with two peptides as negative controls. We used scramb-tat, a membrane-permeant chimeric peptide that does not interfere with the binding of $gp91^{phox}$ to $p47^{phox}$, and gp91ds, which blocks NADPH oxidase in broken cell systems but is impermeant (Rey et al., 2001). As shown in Fig. 7, Cl^- current was elicited with EGF (3.3 nM, 5 min). Then, either scramb-tat (500 nM, 15 min; Fig. 7 A) or gp91ds

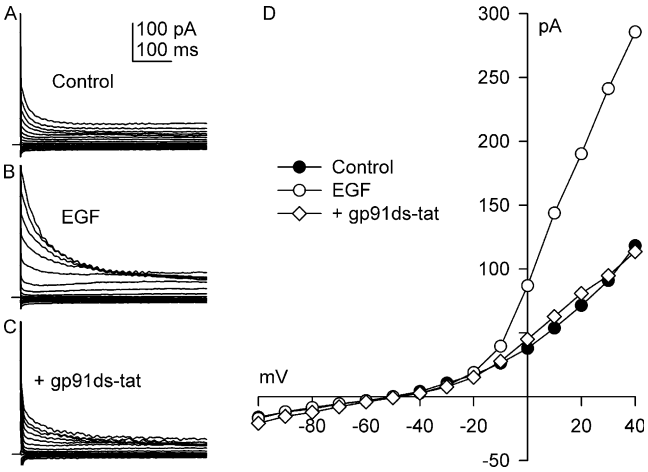

Figure 6. gp91ds-tat, a cell-permeable, chimeric peptide that selectively blocks NADPH oxidase assembly by mimicking the gp91^{phox} docking sequence for p47^{phox}, inhibits EGF-induced Cl^- current. Currents before (A, Control) and after (B, EGF) activation of Cl^- current by EGF (3.3 nM, 5 min), and after exposure to gp91ds-tat (500 nM, 5 min) in the continued presence of EGF (C, +gp91ds-tat). (D) I-V relationships for A–C; each reversed near E_{Cl}. At +40 mV, gp91ds-tat inhibited 133 ± 20% (n = 4, P < 0.001) of the EGF-induced Cl^- current.

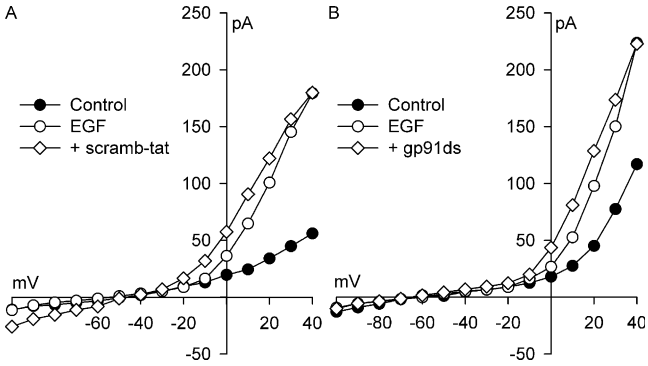

Figure 7. Negative control peptides did not significantly affect EGF-induced Cl^- current. Membrane permeant scramb-tat is a scrambled docking sequence 9-mer fused to the tat 9-mer, and membrane-impermeant gp91ds is the active inhibitory docking sequence 9-mer without tat. (A) I-V relationships before (Control) and after (EGF) exposure to EGF (3.3 nM, 5 min), and after addition of scramb-tat (500 nM, 15 min) in the continued presence of EGF (+scramb-tat). (B) I-V relationships in a separate experiment before (Control) and after (EGF) exposure to EGF (3.3 nM, 5 min), and after addition of gp91ds (500 nM, 15 min) in the continued presence of EGF (+ gp91ds). At +40 mV, scramb-tat and gp91ds inhibited the EGF-induced Cl^- current by −2 ± 7% (n = 4, P = ns) and 7 ± 9% (n = 4, P = ns), respectively.

(500 nM, 15 min; Fig. 7 B) was applied in the continued presence of EGF. Neither negative control peptide suppressed the EGF-induced current. If anything, the currents elicited by EGF continued to increase slightly over most of the voltage range positive to −20 mV. In the experiments with scramb-tat, EGF increased Cl^- current at +40 mV from 1.09 ± 0.22 to 2.03 ± 0.18 pA/pF (n = 4; P < 0.001), and it was 2.04 ± 0.21 pA/pF after a 12–15 min exposure to scramb-tat (n = 4; P = 0.94). Thus, the tat sequence was not sufficient to reproduce the effect of gp91ds-tat. Similarly, in experiments with impermeant gp91ds, EGF increased the Cl^- current at +40 mV from 0.98 ± 0.07 to 1.65 ± 0.04 pA/pF (n = 3; P = 0.001), and it was 1.61 ± 0.02 pA/pF after a 12–15 min exposure to impermeant gp91ds (n = 3; P = 0.57). The ineffectiveness of active but impermeant gp91ds indicates that the site blocked by gp91ds-tat must be in the cytoplasm or on the internal face of the sarcolemma and that gp91ds cannot block the EGF-activated Cl^- channel from the outside.

Cl^- SAC Is a Volume-sensitive Current

Based on its biophysical and pharmacological characteristics, it was hypothesized that the same channel in ventricular myocytes is responsible for both the Cl^- SAC evoked by β1 integrin stretch and the volume-sensitive Cl^- current, $I_{Cl,swell}$ (Browe and Baumgarten, 2003, 2004). Moreover, both Cl^- SAC and $I_{Cl,swell}$ are regulated by several of the same signaling molecules (Browe and Baumgarten, 2003, 2004; Ren and Baumgarten, 2005). If this idea is correct, current elicited by β1 integrin stretch should be volume sensitive. A test of this prediction is illustrated in Fig. 8. After recording control currents in isosmotic 1T bath solution (Fig. 8, A and E), Cl^- SAC was activated by a 5-min integrin stretch in 1T bath solution (Fig. 8, B and E). Suprafusion of 1.5T hyperosmotic bath solution for 10 min while integrin stretch was continued completely inhibited the stretch-induced Cl^- current (Fig. 8, C and E). Moreover, block of the Cl^- SAC by osmotic shrinkage was reversed by returning to 1T bath solution for 5 min while maintaining stretch (Fig. 8, D and E). Inhibition of the Cl^- SAC by osmotic shrinkage was observed in all myocytes studied. Stretch in 1T bath solution increased Cl^- current at +40 mV from 1.10 ± 0.30 to 2.32 ± 0.57 pA/pF (n = 4; P = 0.001), and osmotic shrinkage in 1.5T bath solution (10–12 min) blocked 94 ± 6% (n = 4; P < 0.001) of stretch-activated current, reducing the current at +40 mV to 1.13 ± 0.24 pA/pF, a value not different from control (n = 4; P = 0.91). After reintroduction of 1T bathing solution for 5 min, the current returned to 2.33 ± 0.51 pA/pF, a value not significantly different from that after the initial period of stretch in 1T bathing solution (n = 4; P = 0.95).

The effectiveness of 1.5T in blocking the Cl^- SAC may be overestimated in these experiments because hyperosmotic bath solution also blocks a tamoxifen-sensitive, outwardly rectifying background Cl^- current attributed to partial activation of $I_{Cl,swell}$ under isosmotic conditions (Hume et al., 2000). To estimate the contribution of background $I_{Cl,swell}$ to the current blocked by 1.5T during integrin stretch, unstretched myocytes in 1T were

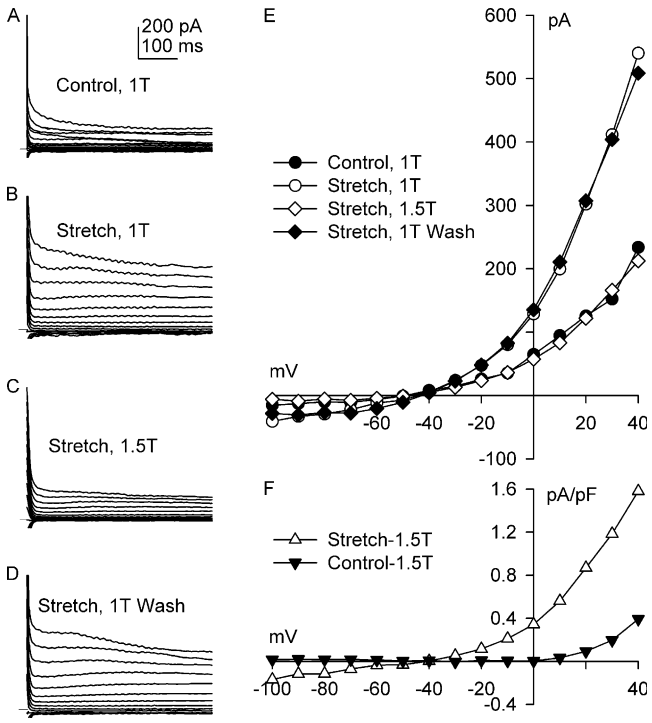

Figure 8. Cl^- SAC and the background current both are volume sensitive and are inhibited by shrinkage in hyperosmotic 1.5T bath solution. Currents before (A; Control, 1T) and after (B; Stretch, 1T) Cl^- SAC activation by integrin stretch (5 min) in 1T bathing solution, after exposure to 1.5T bathing solution (10 min) in the continued presence of stretch (C; Stretch, 1.5T), and after return to 1T bathing solution (5 min) while maintaining stretch (D; Stretch, 1T Wash). (E) I-V relationships for A–D. (F) I-V relationships comparing the osmotic shrinkage-sensitive component of the current after stretch (Stretch-1.5T) and background current (Control-1.5T) in different myocytes. At +40 mV, osmotic shrinkage inhibited 94 ± 6% (n = 4, P < 0.001) of the stretch-induced Cl^- SAC, and the inhibition was reversed upon return to 1T bathing solution (n = 4, P = ns vs. initial 1T, stretch). Furthermore, osmotic shrinkage inhibited 34 ± 4% (n = 4; P = 0.005) of the background current in the absence of stretch.

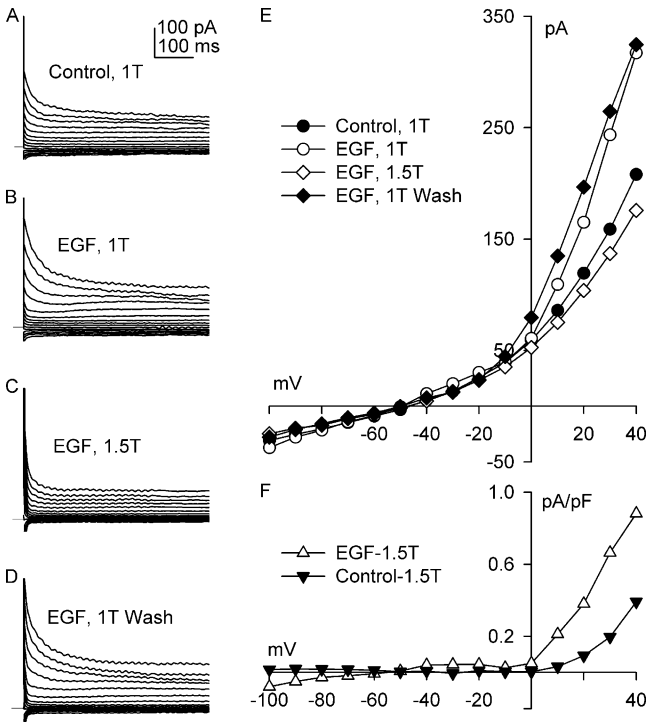

Figure 9. EGF-induced Cl^- current is volume sensitive and is inhibited by shrinkage in hyperosmotic 1.5T bathing solution. Currents before (A; Control, 1T) and after (B; EGF, 1T) activation by EGF (3.3 nM, 5 min) in 1T bathing solution, after exposure to 1.5T bathing solution (10 min) in the continued presence of EGF (C; EGF, 1.5T), and after return to 1T bathing solution (5 min) in the continued presence of EGF (D; EGF, 1T Wash). (E) I-V relationships for A–D. (F) I-V relationships comparing the osmotic shrinkage-sensitive component of the current after EGF (EGF-1.5T) and the background current (Control-1.5T; from Fig. 8 F). At +40 mV, osmotic shrinkage inhibited 127 ± 11% (n = 4, P < 0.001) of the EGF-induced Cl^- current, and the inhibition was reversed upon return to 1T bathing solution containing EGF (n = 4, P = ns vs. initial EGF, 1T).

exposed to 1.5T for 10 min. At +40 mV, osmotic shrinkage in1.5T reduced the background current by 0.53 ± 0.09 pA/pF (n = 4; P = 0.005), from 1.69 ± 0.37 to 1.15 ± 0.29 pA/pF (Fig. 8 F). The current remaining after shrinkage was the same in the absence, 1.15 ± 0.29 pA/pF, and presence, 1.13 ± 0.24 pA/pF, of integrin stretch. On the other hand, the initial background current in the set of cells that were stretched, 1.10 ± 0.30 pA/pF, was smaller than that in the set that was not stretched, 1.69 ± 0.37 pA/pF.

If the EGF-induced Cl^- current is the same as the Cl^- SAC and $I_{Cl,swell}$, it also should be volume sensitive, as is demonstrated in Fig. 9. The Cl^- current in 1T bathing solution (Fig. 9, A and E) was increased by addition of EGF (3.3 nM, 5 min; Fig. 9, B and E). The EGF-induced current was blocked after 10 min of myocyte shrinkage by hyperosmotic 1.5T solution containing EGF (Fig. 9, C and E), and block was completely reversed after returning to 1T bath solution containing EGF for 5 min (Fig. 9, D and E). Fig. 9 F compares the current blocked by 1.5T bathing solution before and after exposure to EGF. At +40 mV, EGF in 1T bathing solution increased the Cl^- current from 1.65 ± 0.19 to 2.32 ± 0.32 pA/pF (n = 4; P = 0.003), and exposure to 1.5T bathing solution with EGF blocked 127 ± 11% (n = 4; P = 0.001) of the EGF-induced current. The current after myocyte shrinkage, 1.46 ± 0.14 pA/pF, was not significantly different than the control current (n = 4; P = 0.22). On returning to 1T bathing solution with EGF, 94 ± 6% (n = 4; P = 0.001) of the initial EGF-induced current recovered; the current recorded under these conditions, 2.25 ± 0.28 pA/pF, was not significantly different from the initial current with EGF (n = 4; P = 0.64).

DISCUSSION

We previously showed that β1 integrin stretch activates an outwardly rectifying, tamoxifen-sensitive Cl^- SAC

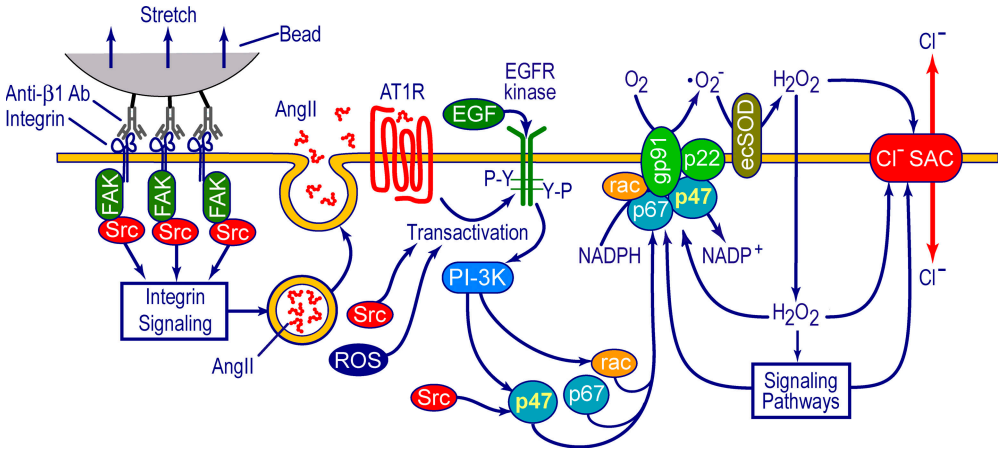

Figure 10. Proposed simplified model of signaling coupling integrin stretch to activation of Cl^- SAC. Integrin stretch activates FAK, Src, and other signaling pathways, which trigger the release of AngII from secretory vesicles. Binding of AngII and/or stretch initiate AT1 receptor signaling, which participates with FAK and Src in the transactivation of EGFR kinase and the subsequent downstream production of PI-3K. Components of these signaling cascades, including PI-3K and Src, induce activation of $p47^{phox}$, $p67^{phox}$, and rac, which translocate to the membrane and assemble with $gp91^{phox}$ and $p22^{phox}$ to form the active NADPH oxidase complex. NADPH oxidase catalyzes the production of $\cdot O_2^-$, which is rapidly converted to H_2O_2 by dismutation. H_2O_2 may activate Cl^- SAC directly or via ROS-sensitive signaling pathways.

under isosmotic conditions via the AngII signaling cascade and involves AT1 receptors, Src/FAK signaling, and H_2O_2 generated, at least in part, by NADPH oxidase (Browe and Baumgarten, 2003, 2004). The present results indicate that EGFR kinase and PI-3K, which couple AT1 receptors to NADPH oxidase (Seshiah et al., 2002), are also components of the signaling cascade that evokes Cl^- SAC in response to integrin stretch. Moreover, stretch- and EGF-induced currents were volume sensitive, suggesting that they are carried by the same channels as $I_{Cl,swell}$.

A simple scheme accounting for both our present and previous findings is depicted in Fig. 10. Activation of Cl^- SAC was abrogated by blockers of EGFR kinase, and exogenous EGF elicited a tamoxifen-sensitive current that mimicked the Cl^- SAC but turned on more rapidly. These data suggest that stretch stimulates Cl^- SAC via EGFR kinase. PI-3K must be downstream from EGFR kinase because inhibition of PI-3K suppressed both the stretch- and EGF-induced current. PI-3K has been implicated in the translocation of Rac to the membrane and the activation of NADPH oxidase (Seshiah et al., 2002; Vignais, 2002). Consistent with this idea, the EGF-induced Cl^- current was blocked by gp91dstat, a selective inhibitor of NADPH oxidase, and we previously demonstrated that stretch-induced Cl^- currents are blocked by other NADPH oxidase inhibitors, diphenyleneiodonium (DPI) and AEBSF (Browe and Baumgarten, 2004). Two other signaling molecules in this cascade, AngII and H_2O_2, also elicit currents that mimic Cl^- SAC in the absence of stretch, whereas the AT1 blocker losartan and degradation of H_2O_2 by catalase inhibit Cl^- SAC (Browe and Baumgarten, 2004). The idea that AT1 receptor activation leads to stimulation of NADPH oxidase by a cascade that includes EGFR kinase and PI-3K is well established in other systems (Seshiah et al., 2002). Although the simple linear scheme in Fig. 10 is sufficient to explain our observations on Cl^- SAC, we cannot exclude additional interactions between these signaling molecules.

Stretch- and osmotic swelling–induced Cl^- currents share several biophysical and pharmacological characteristics, and it has been suggested that Cl^- SAC are carried by the same channels as $I_{Cl,swell}$ (Browe and Baumgarten, 2003, 2004). The present findings support this idea. Both the stretch- and EGF-induced currents were suppressed by osmotic shrinkage, and the EGF-induced current was blocked by tamoxifen, as previously shown for Cl^- SAC (Browe and Baumgarten, 2003).

Cl^- SAC and $I_{Cl,swell}$ also are regulated by some of the same signaling pathways. Block of EGFR kinase inhibits the activation of $I_{Cl,swell}$ by osmotic swelling in human atrial and rabbit ventricular myocytes (Du et al., 2004; Ren and Baumgarten, 2005), and recently we found that AT1 receptors, PI-3K, NADPH oxidase, and ROS play the same roles in eliciting $I_{Cl,swell}$ upon osmotic swelling in rabbit ventricle (Ren et al., 2005) as in response to integrin stretch. In contrast, block of Src family protein tyrosine kinases with PP2 gives a result that depends on the stimulus. PP2 suppresses Cl^- SAC (Browe and Baumgarten, 2003), whereas it stimulates $I_{Cl,swell}$ after it has been activated by swelling (Du et al., 2004; Ren and Baumgarten, 2005; Walsh and Zhang, 2005). Walsh and Zhang (2005) also observed stimulation of $I_{Cl,swell}$ in neonatal rat myocytes when FAK was inhibited by overexpression of FRNK, an endogenous FAK inhibitor. On the other hand, Sorota (1995) found that nonselective tyrosine kinase inhibitors, which also should have inhibited Src and FAK, prevented activation of $I_{Cl,swell}$ in canine atrial myocytes; the reason for this discrepancy is unknown. It is also unclear why inhibition of Src and FAK stimulates $I_{Cl,swell}$ in several preparations but inhibited Cl^- SAC. Osmotic swelling differentially modulates members of the Src

family (Cohen, 2005), whereas PP2 broadly inhibits this protein tyrosine kinase family. Osmotic swelling also may give rise to signaling not elicited by stretch. Other signaling pathways are implicated in the regulation of $I_{Cl,swell}$ (Hume et al., 2000; Baumgarten and Clemo, 2003), but their role in regulation of Cl^- SAC has not been tested.

Although we termed the stretch- and EGF-induced stimulation of Cl^- current an activation, the present studies do not distinguish between de novo opening of channels that are silent in the absence of these stimuli and modulation of $I_{Cl,swell}$ channels that are a major contributor to the background outwardly rectifying Cl^- current under isosmotic conditions (Hume et al., 2000). Block of EGFR kinase by AG1478 and PI-3K by LY 294002 restored stretch- and EGF-induced current to their control level but did not alter the background current in the absence of these stimuli. In contrast, the $I_{Cl,swell}/Cl^-$ SAC blocker tamoxifen and osmotic shrinkage inhibited both the stretch- and EGF-induced and the background current. These observations may suggest that background $I_{Cl,swell}$ is regulated by signaling processes not studied here, but this requires further verification.

Regulation of Cl^- SAC by EGFR Kinase Transactivation and EGF

The ErbB family of receptor tyrosine kinases is represented in mammals by EGFR kinase (ErbB1) and ErbB2–ErbB4, which form homo- and heterodimers (Bogdan and Klämbt, 2001; Holbro and Hynes, 2004). Two lines of evidence implicate EGFR kinase in Cl^- SAC activation. First, 10 μM AG1478 completely blocked Cl^- SAC during stretch, and intracellular pretreatment with a 10-fold lower concentration via the patch pipette suppressed Cl^- SAC activation by subsequent stretch. AG1478 is a highly selective blocker that inhibits ATP binding to EGFR kinase with an IC_{50} of 3 nM, whereas it is a weak inhibitor of ErbB2 and the platelet-derived growth factor receptor with an IC_{50} of >100 μM in both cases (Levitzki and Gazit, 1995). Second, exogenous EGF activated an outwardly rectifying, tamoxifen-sensitive Cl^- current that resembles Cl^- SAC in the absence of stretch. EGF specifically binds to EGFR kinase; ErbB3 and ErbB4 bind neuregulins, and no ligand is known for ErbB2 (Bogdan and Klämbt, 2001; Holbro and Hynes, 2004). While these results clearly implicate EGFR kinase in Cl^- SAC activation, we cannot rule out the possibility that other ErbB family members participate in signaling by forming heterodimers with EGFR kinase.

This appears to be the first evidence that EGFR kinase mediates integrin signaling in cardiac myocytes. Several mechanisms for EGFR kinase transactivation have been identified. Integrins and EGFR colocalize and physically interact within macromolecular complexes at the cell membrane in human ECV304 cells and mouse fibroblasts, and integrin engagement transactivates EGFR kinase in the absence of serum or exogenous growth factors (Moro et al., 2002; Cabodi et al., 2004). This depends on the integrin cytoplasmic tail, the adaptor protein p130Cas, and Src, which phosphorylates EGFR kinase at tyr-845 and triggers autophosphorylation and downstream signaling. In addition, mechanical stretch and AT1 receptors transactivate EGFR kinase by a mechanism that depends on Src and H_2O_2 in a variety of cells (Ushio-Fukai et al., 2001; Oeckler et al., 2003; Kippenberger et al., 2005), and the carboxyl tail of AT1 receptors directly interacts with and transactivates EGFR kinase after phosphorylation of AT1 Y319 (Seta and Sadoshima, 2003). Thus, it is possible that integrin-mediated stretch directly activates EGFR kinase, or a factor directly linked to EGFR kinase activation, in a process that is independent of ligands for this receptor kinase. In this vein, it recently was reported that the AT1 receptor can be activated by stretch by a mechanism independent of AngII binding (Zou et al., 2004).

An autocrine–paracrine mechanism for transactivation of EGFR kinase also is well established in the cardiovascular system (Eguchi et al., 2003; Shah and Catt, 2004). AT1 receptor activation stimulates Zn^{2+}-dependent matrix metalloproteinases (MMPs) that cleave membrane-tethered pro-heparin–binding EGF-like growth factor (proHB-EGF). This causes shedding of soluble heparin-binding EGF (HB-EGF), which is a ligand for EGF kinase. Moreover, integrins bind to and can activate MMP directly (Stanton et al., 1998) and colocalize with proHB-EGF and EGFR kinase at the surface membrane (Nakamura et al., 1995; Moro et al., 2002; Cabodi et al., 2004). Shedding of HB-EGF may explain why the Cl^- current elicited by stretch was about the same magnitude as that activated by exogenous EGF when only a small fraction of the integrins were stretched by magnetic beads. A large number of myocytes with attached beads covered the chamber floor and all were stretched simultaneously. Therefore, the cell under study was exposed to locally released HB-EGF and also to HB-EGF delivered by diffusion and solution flow from other myocytes. Nevertheless, the relative importance of the various mechanisms for transactivation of EGFR kinase is unknown.

Identity of the EGF-induced Cl^- Current

The primary Cl^- currents traditionally recognized in cardiac myocytes include the PKA-dependent Cl^- current due to the cystic fibrosis transmembrane conductance regulator ($I_{CFTR,cardiac}$), the calcium-dependent transient outward Cl^- current ($I_{Cl,Ca}$), and $I_{Cl,swell}$ (Hume et al., 2000). The biophysical and pharmacological profile and volume sensitivity of the EGF-induced Cl^- current are consistent with $I_{Cl,swell}$ rather than either $I_{CFTR,cardiac}$ or $I_{Cl,Ca}$. The EGF-induced Cl^- current and $I_{Cl,swell}$ both activate over several minutes, outwardly rectify, and partially inactivate at positive potentials.

In contrast, $I_{CFTR,cardiac}$ is time independent at all voltages under similar conditions (Hume et al., 2000). $I_{Cl,Ca}$ is activated by cytoplasmic Ca^{2+} transients. With normal Ca^{2+} handling, $I_{Cl,Ca}$ displays outward rectification and inactivates at positive potentials (Zygmunt and Gibbons, 1991). If cytoplasmic Ca^{2+} is clamped at an elevated level, however, $I_{Cl,Ca}$ is time independent. Under the present conditions, $I_{Cl,Ca}$ should be negligible because the bathing solution was Ca^{2+} free, and Ca^{2+} transients were minimized by clamping the cytoplasmic free Ca^{2+} to ~35 nM with 8 mM EGTA. In addition, the EGF-induced Cl^- current was blocked by 10 μM tamoxifen as expected for $I_{Cl,swell}$ (Vandenberg et al., 1994), but $I_{CFTR,cardiac}$ (Vandenberg et al., 1994) and $I_{Cl,Ca}$ (Valverde et al., 1993) are insensitive to tamoxifen. Finally, both EGF-induced Cl^- current and Cl^- SAC were inhibited by myocyte shrinkage with 1.5T hyperosmotic bathing solution. Volume sensitivity is a fundamental characteristic of $I_{Cl,swell}$ that distinguishes it from $I_{CFTR,cardiac}$ and $I_{Cl,Ca}$ (Hume et al., 2000). Thus the characteristics of the EGF-induced Cl^- current resemble $I_{Cl,swell}$. We note, however, that the inward currents observed here are smaller than typical for $I_{Cl,swell}$. EGF elicits larger inward Cl^- currents under different recoding conditions (unpublished data).

EGFR kinase previously was shown to modulate $I_{Cl,swell}$ in human atrial (Du et al., 2004), rabbit ventricular (Ren and Baumgarten, 2005), and cultured neonatal rat ventricular (Walsh and Zhang, 2005) myocytes under different experimental conditions. Moreover, exogenous EGF potentiates $I_{Cl,swell}$ in liver HTC (Varela et al., 2004) and mouse mammary C127 cells (Abdullaev et al., 2003), as well as hypotonicity-induced $^{125}I^-$ flux in human intestine 407 cells (Tilly et al., 1993). In the latter two studies, EGF did not activate anion current under isosmotic conditions, however. EGF also up-regulated $I_{Cl,swell}$ in LNCaP epithelial cells, but this was attributed to enhanced expression of ClC-3 (Lemonnier et al., 2004).

Regulation of Cl^- SAC by PI-3K

Block of integrin stretch- and EGF-induced currents by wortmannin and LY 294002 argues for the participation of PI-3K in the response to both stimuli. Because inhibition of PI-3K suppressed the EGF-induced current, these data also require that PI-3K is downstream from EGFR kinase in the signaling cascade (see Fig. 10), as documented by biochemical methods (Bogdan and Klämbt, 2001). Osmotic activation of $I_{Cl,swell}$ was shown to involve PI-3K in rabbit ventricular myocytes (Ren et al., 2005), smooth muscle (Wang et al., 2004), and epithelial cells (Shi et al., 2002) Moreover, mechanical stretch (Petroff et al., 2001), osmotic swelling (Bewick et al., 1999), integrin activation (Franchini et al., 2000), AngII (Rabkin et al., 1997), and EGFR kinase (Krieg et al., 2004) all stimulate PI-3K in cardiac myocytes.

Cardiac myocytes predominantly express class I PI-3K heterodimers; p110α-p85 is activated by RTK, and p110γ-p101 is activated by the βγ subunits of G proteins (Prasad et al., 2003; Oudit et al., 2004). Wortmannin covalently modifies the p110 catalytic subunit, whereas LY294002 is structurally distinct and competes with ATP for the p110 active site (Stein and Waterfield, 2000; Oudit et al., 2004). The observation that 500 nM wortmannin suppressed only 67% of Cl^- SAC may provide a clue as to which PI-3K isoform is involved. Wortmannin inhibits most PI-3K isoforms with an IC_{50} of 1–10 nM, but monomeric class II PI-3K-C2α, which also is expressed in heart, is relatively insensitive to wortmannin with an IC_{50} of ~400 nM (Stein and Waterfield, 2000; Oudit et al., 2004). The relative insensitivity of the PI-3K-C2α isoform may explain why wortmannin only partially inhibited Cl^- SAC. Consistent with this idea, engagement of integrins activates PI-3K C2α in both platelets (Zhang et al., 1998) and smooth muscle cells (Paulhe et al., 2002). On the other hand, wortmannin, but not LY 294002, augmented the background current in the absence of stretch. The basis for this is unknown, but a stimulation of a background component of current in the presence of stretch would appear as incomplete block of the stretch-induced current. It also must be recognized that neither wortmannin nor LY 294002 is perfectly selective for PI-3K. Wortmannin inhibits myosin light chain kinase, and LY 294002 blocks casein kinase-2, several K^+ channels (Stein and Waterfield, 2000; Oudit et al., 2004), and L-type Ca^{2+} channels (Welling et al., 2005). Because their nonspecific actions differ, however, it seems likely that both antagonists are working here by suppressing the PI-3K pathway. Although there is no evidence to suggest that both wortmannin and LY 294002 block anion channels, we also cannot definitively rule out this possibility.

Regulation of the EGF-induced Cl^- Current by NADPH Oxidase

We previously demonstrated that integrin stretch and AngII elicit Cl^- SAC in ventricular myocytes by activating NADPH oxidase and triggering the production of H_2O_2 (Browe and Baumgarten, 2004). The present results indicate that the EGF-induced current also depends on NADPH oxidase. A membrane-permeant fusion peptide inhibitor of NADPH oxidase assembly, gp91ds-tat, that mimics the docking site on $gp91^{phox}$ for $p47^{phox}$ (Rey et al., 2001) completely blocked Cl^- SAC activation by EGF. In contrast, neither the inactive membrane-permeant fusion peptide scramb-tat nor the active but impermeant gp91ds docking sequence 9-mer altered the EGF-induced current. These results are consistent with the expected intracellular site of action of the docking sequence and rule out nonspecific effects of the tat 9-mer and block of Cl^- channels by gp91ds from the outside. Two recent reports also conclude that exogenous EGF and/or swelling activate $I_{Cl,swell}$ via

NADPH oxidase in HeLa and liver HTC cells based on block of current by DPI (Shimizu et al., 2004; Varela et al., 2004) and expression of the dominant negative $p47^{phox}$ mutant $p47^{S379A}$ (Varela et al., 2004).

An advantage of gp91ds-tat relative to more commonly used NADPH oxidase inhibitors is its specificity, which arises from peptide–peptide interactions. This peptide does not affect the activity of other flavocytochrome enzymes or act as an O_2^- scavenger (Rey et al., 2001). In contrast, DPI, one of the most widely used inhibitors of NADPH oxidase activity, blocks other flavin-containing enzymes, including xanthine oxidase (Doussiere and Vignais, 1992), mitochondrial complex I (Majander et al., 1994), and nitric oxide synthase (Stuehr et al., 1991). Although gp91ds-tat is specific for NADPH oxidase, it apparently does not distinguish between isoforms because the docking sites for $p47^{phox}$ are homologous (Rey et al., 2001). Cardiac myocytes express both the phagocyte-like $gp91^{phox}$ (Nox2) isoform (Li et al., 2002; Xiao et al., 2002; Heymes et al., 2003) and the Nox4 homologue (Byrne et al., 2003). We also cannot rule out the possibility that other sources of ROS are activated by stretch or EGF and participate in the regulation of Cl^- SAC. In preliminary experiments, we found that acetylcholine elicits a tamoxifen-sensitive Cl^- current that is blocked by 5-hydroxydecanoate, implicating mitochondrial K_{ATP} channels or succinate dehydrogenase (Browe and Baumgarten, 2005a), and by rotenone, an inhibitor of mitochondrial complex I (unpublished data).

EGFR kinase and PI-3K participate in the activation of NADPH oxidase and the generation of ROS in response to diverse stimuli in several tissues. Examples include AngII- and prostaglandin $F_{2\alpha}$ receptor–induced hypertrophy of vascular smooth muscle cells (Seshiah et al., 2002; Fan et al., 2005), pressure-induced ROS production in mouse aortic rings (Jung et al., 2004), and exogenous EGF-induced ROS production in Caco-2 and HEK293T cells (Park et al., 2004). Other growth factors, such as PDGF (Marumo et al., 1997) and insulin (Ceolotto et al., 2004), also stimulate NADPH oxidase in nonphagocytic cells by PI-3K signaling. Furthermore, β2 integrin and CD40 engagement elicit NADPH oxidase in leukocytes by a process that requires PI-3K activity (Yamamori et al., 2000; Ha and Lee, 2004).

PI-3K regulates NADPH oxidase assembly and activation by several mechanisms. First, PI-3K leads to phosphorylation of the $p47^{phox}$ subunit, possibly by stimulation of Akt/PKB (Hoyal et al., 2003) or PKC (Yamamori et al., 2000). Second, PtdIns(3,4,5)P_3 and PtdIns(3,4)P_2, the products of PI-3K, bind to PX domains in $p47^{phox}$ and $p40^{phox}$ (Kanai et al., 2001; Zhan et al., 2002), directing these subunits to the plasma membrane. Third, PI-3K stimulates Rac, which also is required for NADPH oxidase assembly (Vignais, 2002). PtdIns(3,4,5)P_3 and PtdIns(3,4)P_2 bind and activate guanine nucleotide exchange factors for Rac and, thereby, trigger Rac activation via GDP–GTP exchange (Park et al., 2004). Finally, H_2O_2 generated by NADPH oxidase feeds forward to potentiate RTK-PI-3K signaling by inhibiting protein tyrosine phosphatases (Knebel et al., 1996; Bae et al., 1997) and the lipid phosphatase PTEN (Rhee et al., 2003), which dephosphorylate the targets of RTK and PI-3K, respectively. H_2O_2 also feeds forward by triggering HB-EGF– (Frank and Eguchi, 2003) and Src-induced (Chen et al., 2001; Sato et al., 2003) EGFR kinase phosphorylation. These actions of H_2O_2 may in part explain its activation of Cl^- SAC in the absence of stretch (Browe and Baumgarten, 2004).

Cl^- SAC Regulation and Cardiac Pathophysiology

HB-EGF, EGFR kinase, PI-3K, NADPH oxidase, and $I_{Cl,swell}$ are concurrently up-regulated in chronic cardiac disease. Exogenous EGF induces hypertrophic responses in ventricular myocytes (Rebsamen et al., 2000). HB-EGF is up-regulated in the peri-infarct region after myocardial infarction (Iwabu et al., 2002), and enhanced expression and activation of HB-EGF and EGFR kinase are key elements of pressure overload– and G protein coupled receptor–induced cardiac hypertrophy (Shah and Catt, 2004; Smith et al., 2004). The Gβγ-regulated p110γisoform of PI-3K is implicated in maladaptive cardiac hypertrophy triggered by both pressure overload and G protein–coupled receptors, and knockout of p110γ prevents heart failure induced by β-adrenergic agonists (Prasad et al., 2003; Oudit et al., 2004). A DPI-sensitive increase in $\cdot O_2^-$ production by myocytes accompanies the development of cardiac hypertrophy and heart failure and is due to increased expression and/or membrane translocation of NADPH oxidase subunits (Li et al., 2002; Heymes et al., 2003). Consistent with the concurrent up-regulation of its regulatory factors, cardiac Cl^- current identified as $I_{Cl,swell}$ is persistently active under isosmotic conditions in cardiac myocytes isolated from rat, rabbit, and canine models of hypertrophy and heart failure and from the peri-infarct zone 30 d after myocardial infarction (Bénitah et al., 1997; Clemo et al., 1999; Baumgarten and Clemo, 2003; c.f., van Borren et al., 2002). Nevertheless, other signaling molecules also may be involved in the regulation of $I_{Cl,swell}$ in cardiac disease.

Limitations

Two limitations of this study should be noted. First, signaling pathways were identified with various agonists and antagonists. Although these agents have been well characterized in the literature, the possibility that nonspecific effects confound our interpretation should be considered. Second, experiments were conducted at a subphysiologic temperature. This may have had a quantitative or even a qualitative impact on the observations.

In summary, β1 integrin stretch elicited Cl^- SAC in ventricular myocytes by transactivation of EGFR kinase and downstream stimulation of PI-3K and NADPH oxidase. Exogenous EGF activated tamoxifen-sensitive Cl^- SAC in the absence of stretch by a process that also involved PI-3K and NADPH oxidase. Furthermore, Cl^- SAC was volume sensitive and was suppressed by osmotic shrinkage in the presence of stretch or EGF. Thus, it is likely that the Cl^- SAC is mediated by the same channel as $I_{Cl,swell}$.

We thank Steven E. Hutchens for technical assistance.

This work was supported by grants HL46764 and HL65435 from the National Institutes of Health.

Olaf S. Andersen served as editor.

Submitted: 15 July 2005
Accepted: 27 January 2006

REFERENCES

Abdullaev, I.F., R.Z. Sabirov, and Y. Okada. 2003. Upregulation of swelling-activated Cl^- channel sensitivity to cell volume by activation of EGF receptors in murine mammary cells. *J. Physiol.* 549:749–758.

Bae, Y.S., S.W. Kang, M.S. Seo, I.C. Baines, E. Tekle, P.B. Chock, and S.G. Rhee. 1997. Epidermal growth factor (EGF)-induced generation of hydrogen peroxide. Role in EGF receptor-mediated tyrosine phosphorylation. *J. Biol. Chem.* 272:217–221.

Baumgarten, C.M., and H.F. Clemo. 2003. Swelling-activated chloride channels in cardiac physiology and pathophysiology. *Prog. Biophys. Mol. Biol.* 82:25–42.

Bénitah, J.-P., A.M. Gomez, C. Delgado, P. Lorente, and W.J. Lederer. 1997. A chloride current component induced by hypertrophy in rat ventricular myocytes. *Am. J. Physiol.* 272:H2500–H2506.

Bewick, N.L., C. Fernandes, A.D. Pitt, H.H. Rasmussen, and D.W. Whalley. 1999. Mechanisms of Na^+-K^+ pump regulation in cardiac myocytes during hyposmolar swelling. *Am. J. Physiol.* 276: C1091–C1099.

Bogdan, S., and C. Klämbt. 2001. Epidermal growth factor receptor signaling. *Curr. Biol.* 11:R292–R295.

Browe, D.M., and C.M. Baumgarten. 2003. Stretch of β1 integrin activates an outwardly rectifying chloride current via FAK and Src in rabbit ventricular myocytes. *J. Gen. Physiol.* 122:689–702.

Browe, D.M., and C.M. Baumgarten. 2004. Angiotensin II (AT1) receptors and NADPH oxidase regulate Cl^- current elicited by β1 integrin stretch in rabbit ventricular myocytes. *J. Gen. Physiol.* 124:273–287.

Browe, D.M., and C.M. Baumgarten. 2005a. Acetylcholine activates the swelling-activated chloride current, $I_{Cl,swell}$ in rabbit ventricular myocytes by opening mitochondrial K_{ATP} channels. *Biophys. J.* 88:289a (Abstr.).

Browe, D.M., and C.M. Baumgarten. 2005b. Stretch of β1 integrin elicits swelling-activated Cl current via transactivation of EGFR, phosphatidylinositol-3-kinase and NADPH oxidase in rabbit ventricular myocytes. *Biophys. J.* 88:289a (Abstr.).

Brunton, V.G., B.W. Ozanne, C. Paraskeva, and M.C. Frame. 1997. A role for epidermal growth factor receptor, c-Src and focal adhesion kinase in an in vitro model for the progression of colon cancer. *Oncogene.* 14:283–293.

Byrne, J.A., D.J. Grieve, J.K. Bendall, J.M. Li, C. Gove, J.D. Lambeth, A.C. Cave, and A.M. Shah. 2003. Contrasting roles of NADPH oxidase isoforms in pressure-overload versus angiotensin II-induced cardiac hypertrophy. *Circ. Res.* 93:802–805.

Cabodi, S., L. Moro, E. Bergatto, E.E. Boeri, P. Di Stefano, E. Turco, G. Tarone, and P. Defilippi. 2004. Integrin regulation of epidermal growth factor (EGF) receptor and of EGF-dependent responses. *Biochem. Soc. Trans.* 32:438–442.

Ceolotto, G., M. Bevilacqua, I. Papparella, E. Baritono, L. Franco, C. Corvaja, M. Mazzoni, A. Semplicini, and A. Avogaro. 2004. Insulin generates free radicals by an NAD(P)H, phosphatidylinositol 3′-kinase-dependent mechanism in human skin fibroblasts ex vivo. *Diabetes.* 53:1344–1351.

Chen, K., J.A. Vita, B.C. Berk, and J.F. Keaney Jr. 2001. c-Jun N-terminal kinase activation by hydrogen peroxide in endothelial cells involves SRC-dependent epidermal growth factor receptor transactivation. *J. Biol. Chem.* 276:16045–16050.

Clemo, H.F., B.S. Stambler, and C.M. Baumgarten. 1999. Swelling-activated chloride current is persistently activated in ventricular myocytes from dogs with tachycardia-induced congestive heart failure. *Circ. Res.* 84:157–165.

Cohen, D.M. 2005. SRC family kinases in cell volume regulation. *Am. J. Physiol. Cell Physiol.* 288:C483–C493.

Doussiere, J., and P.V. Vignais. 1992. Diphenylene iodonium as an inhibitor of the NADPH oxidase complex of bovine neutrophils. Factors controlling the inhibitory potency of diphenylene iodonium in a cell-free system of oxidase activation. *Eur. J. Biochem.* 208:61–71.

Du, X.L., Z. Gao, C.P. Lau, S.W. Chiu, H.F. Tse, C.M. Baumgarten, and G.R. Li. 2004. Differential effects of tyrosine kinase inhibitors on volume-sensitive chloride current in human atrial myocytes: evidence for dual regulation by Src and EGFR kinases. *J. Gen. Physiol.* 123:427–439.

Eguchi, S., G.D. Frank, M. Mifune, and T. Inagami. 2003. Metalloprotease-dependent ErbB ligand shedding in mediating EGFR transactivation and vascular remodelling. *Biochem. Soc. Trans.* 31:1198–1202.

Fan, C., M. Katsuyama, T. Nishinaka, and C. Yabe-Nishimura. 2005. Transactivation of the EGF receptor and a PI3 kinase-ATF-1 pathway is involved in the upregulation of NOX1, a catalytic subunit of NADPH oxidase. *FEBS Lett.* 579:1301–1305.

Franchini, K.G., A.S. Torsoni, P.H. Soares, and M.J. Saad. 2000. Early activation of the multicomponent signaling complex associated with focal adhesion kinase induced by pressure overload in the rat heart. *Circ. Res.* 87:558–565.

Frank, G.D., and S. Eguchi. 2003. Activation of tyrosine kinases by reactive oxygen species in vascular smooth muscle cells: significance and involvement of EGF receptor transactivation by angiotensin II. *Antioxid. Redox Signal.* 5:771–780.

Gauss, K.A., P.L. Mascolo, D.W. Siemsen, L.K. Nelson, P.L. Bunger, P.J. Pagano, and M.T. Quinn. 2002. Cloning and sequencing of rabbit leukocyte NADPH oxidase genes reveals a unique $p67^{phox}$ homolog. *J. Leukoc. Biol.* 71:319–328.

Ha, Y.J., and J.R. Lee. 2004. Role of TNF receptor-associated factor 3 in the CD40 signaling by production of reactive oxygen species through association with $p40^{phox}$, a cytosolic subunit of nicotinamide adenine dinucleotide phosphate oxidase. *J. Immunol.* 172:231–239.

Heymes, C., J.K. Bendall, P. Ratajczak, A.C. Cave, J.L. Samuel, G. Hasenfuss, and A.M. Shah. 2003. Increased myocardial NADPH oxidase activity in human heart failure. *J. Am. Coll. Cardiol.* 41:2164–2171.

Holbro, T., and N.E. Hynes. 2004. ErbB receptors: directing key signaling networks throughout life. *Annu. Rev. Pharmacol. Toxicol.* 44:195–217.

Hoyal, C.R., A. Gutierrez, B.M. Young, S.D. Catz, J.H. Lin, P.N. Tsichlis, and B.M. Babior. 2003. Modulation of $p47^{PHOX}$ activity by site-specific phosphorylation: Akt-dependent activation of the NADPH oxidase. *Proc. Natl. Acad. Sci. USA.* 100:5130–5135.

Hume, J.R., D. Duan, M.L. Collier, J. Yamazaki, and B. Horowitz. 2000. Anion transport in heart. *Physiol. Rev.* 80:31–81.

Iwabu, A., T. Murakami, S. Kusachi, K. Nakamura, S. Takemoto, I. Komatsubara, S. Sezaki, J. Hayashi, Y. Ninomiya, and T. Tsuji. 2002. Concomitant expression of heparin-binding epidermal growth factor-like growth factor mRNA and basic fibroblast growth factor mRNA in myocardial infarction in rats. *Basic Res. Cardiol.* 97:214–222.

Jung, O., J.G. Schreiber, H. Geiger, T. Pedrazzini, R. Busse, and R.P. Brandes. 2004. gp91phox-containing NADPH oxidase mediates endothelial dysfunction in renovascular hypertension. *Circulation.* 109:1795–1801.

Kanai, F., H. Liu, S.J. Field, H. Akbary, T. Matsuo, G.E. Brown, L.C. Cantley, and M.B. Yaffe. 2001. The PX domains of p47phox and p40phox bind to lipid products of PI(3)K. *Nat. Cell Biol.* 3:675–678.

Kippenberger, S., S. Loitsch, M. Guschel, J. Muller, Y. Knies, R. Kaufmann, and A. Bernd. 2005. Mechanical stretch stimulates protein kinase B/Akt phosphorylation in epidermal cells via angiotensin II type 1 receptor and epidermal growth factor receptor. *J. Biol. Chem.* 280:3060–3067.

Knebel, A., H.J. Rahmsdorf, A. Ullrich, and P. Herrlich. 1996. Dephosphorylation of receptor tyrosine kinases as target of regulation by radiation, oxidants or alkylating agents. *EMBO J.* 15:5314–5325.

Krieg, T., L. Cui, Q. Qin, M.V. Cohen, and J.M. Downey. 2004. Mitochondrial ROS generation following acetylcholine-induced EGF receptor transactivation requires metalloproteinase cleavage of proHB-EGF. *J. Mol. Cell. Cardiol.* 36:435–443.

Lemonnier, L., Y. Shuba, A. Crepin, M. Roudbaraki, C. Slomianny, B. Mauroy, B. Nilius, N. Prevarskaya, and R. Skryma. 2004. Bcl-2-dependent modulation of swelling-activated Cl^- current and ClC-3 expression in human prostate cancer epithelial cells. *Cancer Res.* 64:4841–4848.

Levitzki, A., and A. Gazit. 1995. Tyrosine kinase inhibition: an approach to drug development. *Science.* 267:1782–1788.

Li, J.M., N.P. Gall, D.J. Grieve, M. Chen, and A.M. Shah. 2002. Activation of NADPH oxidase during progression of cardiac hypertrophy to failure. *Hypertension.* 40:477–484.

Majander, A., M. Finel, and M. Wikstrom. 1994. Diphenyleneiodonium inhibits reduction of iron-sulfur clusters in the mitochondrial NADH-ubiquinone oxidoreductase (Complex I). *J. Biol. Chem.* 269:21037–21042.

Marumo, T., V.B. Schini-Kerth, B. Fisslthaler, and R. Busse. 1997. Platelet-derived growth factor-stimulated superoxide anion production modulates activation of transcription factor NF-κB and expression of monocyte chemoattractant protein 1 in human aortic smooth muscle cells. *Circulation.* 96:2361–2367.

Moro, L., L. Dolce, S. Cabodi, E. Bergatto, E.B. Erba, M. Smeriglio, E. Turco, S.F. Retta, M.G. Giuffrida, M. Venturino, et al. 2002. Integrin-induced epidermal growth factor (EGF) receptor activation requires c-Src and p130Cas and leads to phosphorylation of specific EGF receptor tyrosines. *J. Biol. Chem.* 277:9405–9414.

Prasad, S.V., C. Perrino, and H.A. Rockman. 2003. Role of phosphoinositide 3-kinase in cardiac function and heart failure. *Trends Cardiovasc. Med.* 13:206–212.

Nakamura, K., R. Iwamoto, and E. Mekada. 1995. Membrane-anchored heparin-binding EGF-like growth factor (HB-EGF) and diphtheria toxin receptor-associated protein (DRAP27)/CD9 form a complex with integrin α3 β1 at cell–cell contact sites. *J. Cell Biol.* 129:1691–1705.

Oeckler, R.A., P.M. Kaminski, and M.S. Wolin. 2003. Stretch enhances contraction of bovine coronary arteries via an NAD(P)H oxidase-mediated activation of the extracellular signal-regulated kinase mitogen-activated protein kinase cascade. *Circ. Res.* 92:23–31.

Oudit, G.Y., H. Sun, B.G. Kerfant, M.A. Crackower, J.M. Penninger, and P.H. Backx. 2004. The role of phosphoinositide-3 kinase and PTEN in cardiovascular physiology and disease. *J. Mol. Cell. Cardiol.* 37:449–471.

Park, H.S., S.H. Lee, D. Park, J.S. Lee, S.H. Ryu, W.J. Lee, S.G. Rhee, and Y.S. Bae. 2004. Sequential activation of phosphatidylinositol 3-kinase, βPix, Rac1, and Nox1 in growth factor-induced production of H_2O_2. *Mol. Cell. Biol.* 24:4384–4394.

Paulhe, F., B. Perret, H. Chap, N. Iberg, O. Morand, and C. Racaud-Sultan. 2002. Phosphoinositide 3-kinase C2α is activated upon smooth muscle cell migration and regulated by $\alpha_v\beta_3$ integrin engagement. *Biochem. Biophys. Res. Commun.* 297:261–266.

Petroff, M.G., S.H. Kim, S. Pepe, C. Dessy, E. Marban, J.L. Balligand, and S.J. Sollott. 2001. Endogenous nitric oxide mechanisms mediate the stretch dependence of Ca^{2+} release in cardiomyocytes. *Nat. Cell Biol.* 3:867–873.

Rabkin, S.W., V. Goutsouliak, and J.Y. Kong. 1997. Angiotensin II induces activation of phosphatidylinositol 3-kinase in cardiomyocytes. *J. Hypertens.* 15:891–899.

Rebsamen, M.C., J.F. Arrighi, C.E. Juge-Aubry, M.B. Vallotton, and U. Lang. 2000. Epidermal growth factor induces hypertrophic responses and Stat5 activation in rat ventricular cardiomyocytes. *J. Mol. Cell. Cardiol.* 32:599–610.

Ren, Z., and C.M. Baumgarten. 2005. Antagonistic regulation of swelling-activated chloride current in rabbit ventricle by Src and EGFR protein tyrosine kinases. *Am. J. Physiol. Heart Circ. Physiol.* 288:H2628–H2636.

Ren, Z., D.M. Browe, and C.M. Baumgarten. 2005. Regulation of swelling-activated chloride current by angiotensin AT1 receptors, EGFR kinase, Src, and NADPH oxidase in rabbit ventricular myocytes. *Biophys. J.* 88:290a (Abstr.).

Rey, F.E., M.E. Cifuentes, A. Kiarash, M.T. Quinn, and P.J. Pagano. 2001. Novel competitive inhibitor of NAD(P)H oxidase assembly attenuates vascular O_2^- and systolic blood pressure in mice. *Circ. Res.* 89:408–414.

Rhee, S.G., S.-R. Lee, K.-S. Yang, J. Kwon, and S.W. Kang. 2003. Hydrogen peroxide as intracellular messenger: identification of protein tyrosine phosposphatases and PTEN as H_2O_2 target. *In* Signal Transduction by Reactive Oxygen and Nitrogen Species: Pathways and Chemical Principles. H.J. Forman, J. Fukuto, and M. Torres, editors. Kluwer, Dordrect. 167–179.

Sadoshima, J., and S. Izumo. 1997. The cellular and molecular response of cardiac myocytes to mechanical stress. *Annu. Rev. Physiol.* 59:551–571.

Sato, K., T. Nagao, T. Iwasaki, Y. Nishihira, and Y. Fukami. 2003. Src-dependent phosphorylation of the EGF receptor Tyr-845 mediates Stat-$p21^{waf1}$ pathway in A431 cells. *Genes Cells.* 8:995–1003.

Seshiah, P.N., D.S. Weber, P. Rocic, L. Valppu, Y. Taniyama, and K.K. Griendling. 2002. Angiotensin II stimulation of NAD(P)H oxidase activity: upstream mediators. *Circ. Res.* 91:406–413.

Seta, K., and J. Sadoshima. 2003. Phosphorylation of tyrosine 319 of the angiotensin II type 1 receptor mediates angiotensin II-induced trans-activation of the epidermal growth factor receptor. *J. Biol. Chem.* 278:9019–9026.

Shah, B.H. 2002. Epidermal growth factor receptor transactivation in angiotensin II-induced signaling: role of cholesterol-rich microdomains. *Trends Endocrinol. Metab.* 13:1–2.

Shah, B.H., and K.J. Catt. 2003. A central role of EGF receptor transactivation in angiotensin II -induced cardiac hypertrophy. *Trends Pharmacol. Sci.* 24:239–244.

Shah, B.H., and K.J. Catt. 2004. Matrix metalloproteinase-dependent EGF receptor activation in hypertension and left ventricular hypertrophy. *Trends Endocrinol. Metab.* 15:241–243.

Shi, C., S. Barnes, M. Coca-Prados, and M.E. Kelly. 2002. Protein tyrosine kinase and protein phosphatase signaling pathways

regulate volume-sensitive chloride currents in a nonpigmented ciliary epithelial cell line. *Invest. Ophthalmol. Vis. Sci.* 43:1525–1532.

Shimizu, T., T. Numata, and Y. Okada. 2004. A role of reactive oxygen species in apoptotic activation of volume-sensitive Cl^- channel. *Proc. Natl. Acad. Sci. USA.* 101:6770–6773.

Smith, N.J., H.W. Chan, J.E. Osborne, W.G. Thomas, and R.D. Hannan. 2004. Hijacking epidermal growth factor receptors by angiotensin II: new possibilities for understanding and treating cardiac hypertrophy. *Cell. Mol. Life Sci.* 61:2695–2703.

Sorota, S. 1992. Swelling-induced chloride-sensitive current in canine atrial cells revealed by whole-cell patch-clamp method. *Circ. Res.* 70:679–687.

Sorota, S. 1995. Tyrosine protein kinase inhibitors prevent activation of cardiac swelling-induced chloride current. *Pflugers Arch.* 431:178–185.

Stanton, H., J. Gavrilovic, S.J. Atkinson, M.P. d'Ortho, K.M. Yamada, L. Zardi, and G. Murphy. 1998. The activation of ProMMP-2 (gelatinase A) by HT1080 fibrosarcoma cells is promoted by culture on a fibronectin substrate and is concomitant with an increase in processing of MT1-MMP (MMP-14) to a 45 kDa form. *J. Cell Sci.* 111:2789–2798.

Stein, R.C., and M.D. Waterfield. 2000. PI3-kinase inhibition: a target for drug development? *Mol. Med. Today.* 6:347–357.

Stuehr, D.J., O.A. Fasehun, N.S. Kwon, S.S. Gross, J.A. Gonzalez, R. Levi, and C.F. Nathan. 1991. Inhibition of macrophage and endothelial cell nitric oxide synthase by diphenyleneiodonium and its analogs. *FASEB J.* 5:98–103.

Tilly, B.C., N. van den Berghe, L.G. Tertoolen, M.J. Edixhoven, and H.R. de Jonge. 1993. Protein tyrosine phosphorylation is involved in osmoregulation of ionic conductances. *J. Biol. Chem.* 268:19919–19922.

Tseng, G.-N. 1992. Cell swelling increases membrane conductance of canine cardiac cells: evidence for a volume-sensitive Cl channel. *Am. J. Physiol.* 262:C1056–C1068.

Ushio-Fukai, M., R.W. Alexander, M. Akers, Q. Yin, Y. Fujio, K. Walsh, and K.K. Griendling. 1999. Reactive oxygen species mediate the activation of Akt/protein kinase B by angiotensin II in vascular smooth muscle cells. *J. Biol. Chem.* 274:22699–22704.

Ushio-Fukai, M., K.K. Griendling, P.L. Becker, L. Hilenski, S. Halleran, and R.W. Alexander. 2001. Epidermal growth factor receptor transactivation by angiotensin II requires reactive oxygen species in vascular smooth muscle cells. *Arterioscler. Thromb. Vasc. Biol.* 21:489–495.

Valverde, M.A., G.M. Mintenig, and F.V. Sepulveda. 1993. Differential effects of tamoxifen and I^- on three distinguishable chloride currents activated in T84 intestinal cells. *Pflugers Arch.* 425:552–554.

van Borren, M.M., A.O. Verkerk, S.K. Vanharanta, A. Baartscheer, R. Coronel, and J.H. Ravesloot. 2002. Reduced swelling-activated Cl^- current densities in hypertrophied ventricular myocytes of rabbits with heart failure. *Cardiovasc. Res.* 53:869–878.

Vandenberg, J.I., A. Yoshida, K. Kirk, and T. Powell. 1994. Swelling-activated and isoprenaline-activated chloride currents in guinea pig cardiac myocytes have distinct electrophysiology and pharmacology. *J. Gen. Physiol.* 104:997–1017.

Varela, D., F. Simon, A. Riveros, F. Jorgensen, and A. Stutzin. 2004. NAD(P)H oxidase-derived H_2O_2 signals chloride channel activation in cell volume regulation and cell proliferation. *J. Biol. Chem.* 279:13301–13304.

Vignais, P.V. 2002. The superoxide-generating NADPH oxidase: structural aspects and activation mechanism. *Cell. Mol. Life Sci.* 59:1428–1459.

Walsh, K.B., and J. Zhang. 2005. Regulation of cardiac volume-sensitive chloride channel by focal adhesion kinase and Src kinase. *Am. J. Physiol. Heart Circ. Physiol.* 289:H2566–H2574.

Wang, G.X., C. McCrudden, Y.P. Dai, B. Horowitz, J.R. Hume, and I.A. Yamboliev. 2004. Hypotonic activation of volume-sensitive outwardly rectifying chloride channels in cultured PASMCs is modulated by SGK. *Am. J. Physiol. Heart Circ. Physiol.* 287:H533–H544.

Welling, A., F. Hofmann, and J.W. Wegener. 2005. Inhibition of L-type Cav1.2 Ca^{2+} channels by 2,(4-morpholinyl)-8-phenyl-4H-1-benzopyran-4-one (LY294002) and 2-[1-(3-dimethyl- aminopropyl)-5-methoxyindol-3-yl]-3-(1H-indol-3-yl) maleimide (Go6983). *Mol. Pharmacol.* 67:541–544.

Xiao, L., D.R. Pimentel, J. Wang, K. Singh, W.S. Colucci, and D.B. Sawyer. 2002. Role of reactive oxygen species and NAD(P)H oxidase in α_1-adrenoceptor signaling in adult rat cardiac myocytes. *Am. J. Physiol. Cell Physiol.* 282:C926–C934.

Yamamori, T., O. Inanami, H. Nagahata, Y. Cui, and M. Kuwabara. 2000. Roles of p38 MAPK, PKC and PI3-K in the signaling pathways of NADPH oxidase activation and phagocytosis in bovine polymorphonuclear leukocytes. *FEBS Lett.* 467:253–258.

Zhan, Y., J.V. Virbasius, X. Song, D.P. Pomerleau, and G.W. Zhou. 2002. The p40*phox* and p47*phox* PX domains of NADPH oxidase target cell membranes via direct and indirect recruitment by phosphoinositides. *J. Biol. Chem.* 277:4512–4518.

Zhang, J., H. Banfic, F. Straforini, L. Tosi, S. Volinia, and S.E. Rittenhouse. 1998. A type II phosphoinositide 3-kinase is stimulated via activated integrin in platelets. A source of phosphatidylinositol 3-phosphate. *J. Biol. Chem.* 273:14081–14084.

Zhidkova, N.I., A.M. Belkin, and R. Mayne. 1995. Novel isoform of β1 integrin expressed in skeletal and cardiac muscle. *Biochem. Biophys. Res. Commun.* 214:279–285.

Zou, Y., H. Akazawa, Y. Qin, M. Sano, H. Takano, T. Minamino, N. Makita, K. Iwanaga, W. Zhu, S. Kudoh, et al. 2004. Mechanical stress activates angiotensin II type 1 receptor without the involvement of angiotensin II. *Nat. Cell Biol.* 6:499–506.

Zygmunt, A.C., and W.R. Gibbons. 1991. Calcium-activated chloride current in rabbit ventricular myocytes. *Circ. Res.* 68:424–437.